Cell Reports, Volume *32*

Supplemental Information

Intraflagellar Transport Complex B Proteins Regulate the Hippo Effector Yap1 during Cardiogenesis

Marina Peralta, Laia Ortiz Lopez, Katerina Jerabkova, Tommaso Lucchesi, Benjamin Vitre, Dong Han, Laurent Guillemot, Chaitanya Dingare, Izabela Sumara, Nadia Mercader, Virginie Lecaudey, Benedicte Delaval, Sigolène M. Meilhac, and Julien Vermot

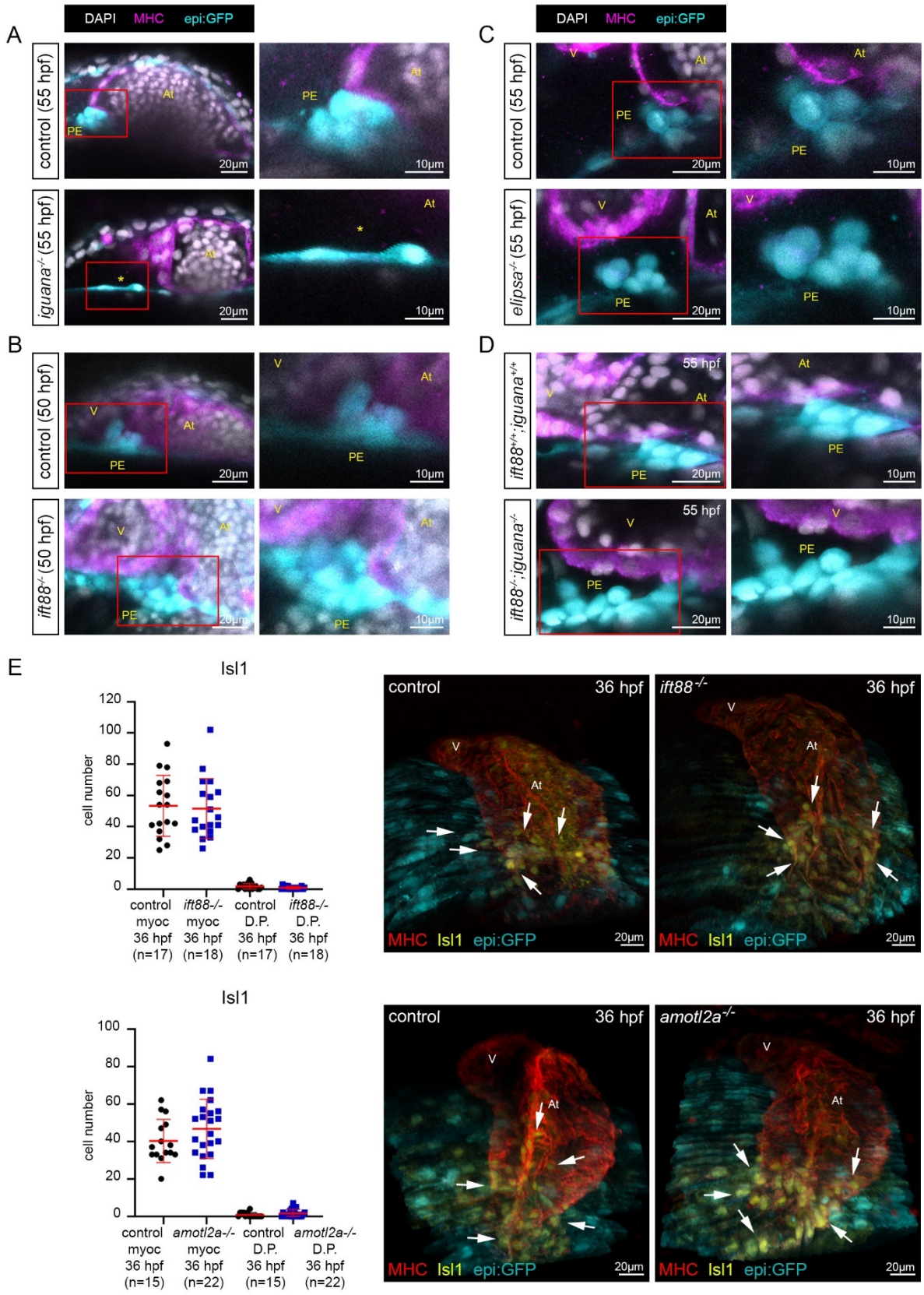
A
DAPI MHC epi:GFP
control (55 hpf)
iguana-/- (55 hpf)
At
PE
V
*
20µm
10µm
B
control (50 hpf)
ift88-/- (50 hpf)
C
elipsa-/- (55 hpf)
D
ift88+/+;iguana+/+
ift88-/-;iguana-/-
55 hpf
E
Isl1
cell number
control myoc 36 hpf (n=17)
ift88-/- myoc 36 hpf (n=18)
control D.P. 36 hpf (n=17)
ift88-/- D.P. 36 hpf (n=18)
amotl2a-/- myoc 36 hpf (n=22)
amotl2a-/- D.P. 36 hpf (n=15)
amotl2a-/- D.P. 36 hpf (n=22)
control 36 hpf
ift88-/- 36 hpf
amotl2a-/- 36 hpf
MHC Isl1 epi:GFP

Figure S1. IFT complex B mutants show increased proepicardial size without affecting Islet1 cell number in zebrafish. Related to Figures 1 and 2.

(A-D) *Confocal sections of whole mount immunofluorescence (IF) of iguana$^{-/-}$, epi:GFP* ***(A)****, ift88$^{-/-}$, epi:GFP* ***(B)****, elipsa$^{-/-}$, epi:GFP* ***(C)*** *and ift88$^{-/-}$, iguana$^{-/-}$, epi:GFP* ***(D)*** *and their controls using anti-myosin heavy chain antibody (MHC) (magenta), anti-GFP (cyan) and DAPI (white) antibodies. Asterisk shows lack of avcPE as there is only one rounded PE cell. Zoomed regions contained inside the red boxes are showed on the right side.* ***(E)*** *The top graph shows number of Isl1-positive cells in the myocardium and dorsal pericardium (D.P.) quantified in ift88-/-, epi:GFP (n=18) and control (n=17) embryos at 36 hpf (t-test myocardium p value 0.785 and Mann Whitney test D.P. p value 0.216). Bottom graph shows number of Isl1-positive cells in the myocardium and D.P. quantified in amotl2a-/-, epi:GFP (n=15) and control (n=22) embryos at 36 hpf (t-test myocardium p value 0.188 and Mann Whitney test D.P. p value 0.167). In all graphs, red bars indicate mean ± standard deviation. 3D projections of whole mount IF of hearts using MHC (red), epi:GFP (cyan) and Isl1 (yellow) antibody. White arrows mark Isl –positive cells. All images are ventral views, anterior is to the top. V, ventricle; At, atrium; PE, avcPE.*

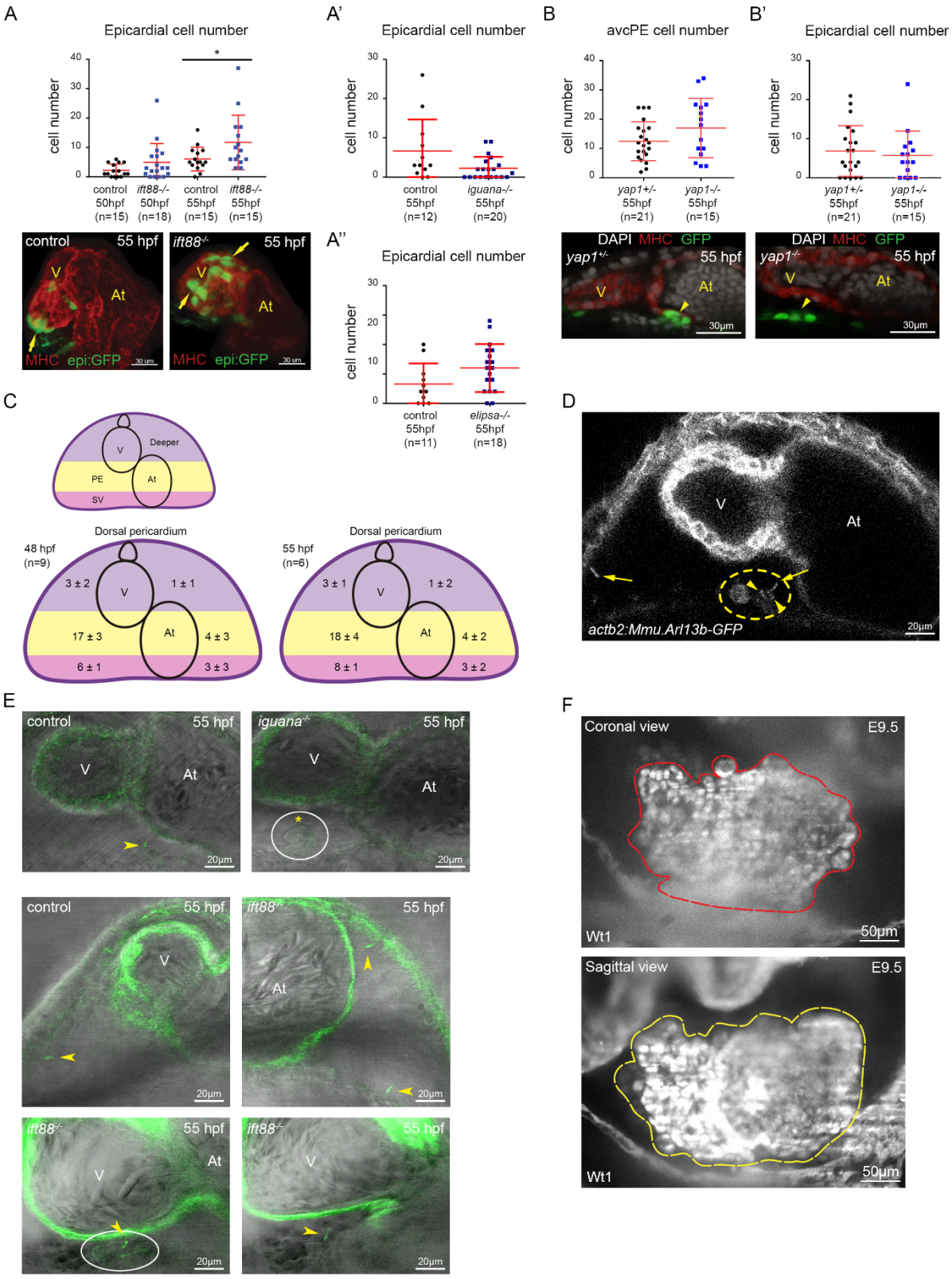

Figure S2. Cilia protruding into the pericardial cavity are distributed heterogeneously in zebrafish during proepicardial development. Related to Figures 1 and 3 and STAR methods.

(A-A'') *Graphs show epicardial cell numbers quantified in ift88, iguana and elipsa mutants in epi:GFP background.* ***(A)*** *At 55 hpf, ift88 mutants (n=15) showed increased epicardial cell numbers (t-test p value 0.04). 3D projections of whole mount immunofluorescence (IF) of hearts using anti-myosin heavy chain antibody (MHC) (red) and GFP (green) expression. Arrows mark some epicardial cells;* ***(A')*** *iguana mutants (n=20) showed a tendency towards decreased epicardial cell numbers (t-test p value 0.055), while* ***(A'')*** *elipsa mutants (n=18) showed a tendency towards increased epicardial cell number (t-test p value 0.08).* ***(B)*** *Graph shows avcPE cell numbers quantified in yap1$^{-/-}$ (n=15) and control (n=21) embryos in tcf21:nsl-GFP background at 55 hpf. (t-test p-value 0.12) Control and yap1$^{-/-}$ IF confocal sections labelled with MHC (red), GFP (green), DAPI (white). Yellow arrowheads point at the avcPE.* ***(B')*** *Graph shows epicardial cell numbers quantified in yap1$^{-/-}$ (n=15) and control (n=21) embryos in tcf21:nsl-GFP background at 55 hpf. (Mann Whitney p-value 0.63)* ***(C)*** *For cilia quantification, we divided the dorsal pericardial wall in to three different regions: SV region, including the sinus venosus (pink); PE region, where the avcPE forms (yellow) and Deeper region (purple). These three regions were subdivided in to right and left halves, containing the ventricle or the atrium respectively. At 48 hpf (n=9 larvae), prior to PE formation, cilia protruding from the dorsal pericardium showed a heterogeneous distribution. Interestingly, the right half of the SV (6 ± 1) and the PE (17 ± 3) regions, where both PE clusters will form, presented higher cilia number than the rest of the regions. At 55 hpf, when the avcPE is formed, the cilia distribution was similar to that observed at 48 hpf (n= 6 larvae).* ***(D)*** *Confocal section of actb2:Mmu.Arl13b-GFP embryo (55 hpf). Yellow dotted circle encloses the avcPE. Yellow arrows point to cilia protruding from the ventral and dorsal pericardium. Yellow arrowheads point at immotile and bent cilia protruding from a few avcPE cells.* ***(E)*** *Confocal sections of iguana; actb2:Mmu.Arl13b-GFP, ift88; actb2:Mmu.Arl13b-GFP and control embryos. In controls, yellow arrowhead points at cilium protruding into the*

pericardial cavity. In iguana yellow asterisk shows lack of cilia in the avcPE (enclosed in the white circle). Confocal section of ift88; actb2:Mmu.Arl13b-GFP and control embryos. In ift88 mutant embryo, yellow arrowheads point at cilia protruding from ventral and dorsal pericardium and the avcPE (enclosed in the white circle). ***(F)*** *Coronal and sagittal sections acquired by light sheet microscopy to illustrate the methods used to measure PE volume (labeled with anti-Wt1 antibody). Red and yellow dotted shapes enclose the PE area. In all the images ventral views, anterior is to the top. V, ventricle; At, atrium. In all graphs, red bars indicate mean ± standard deviation.*

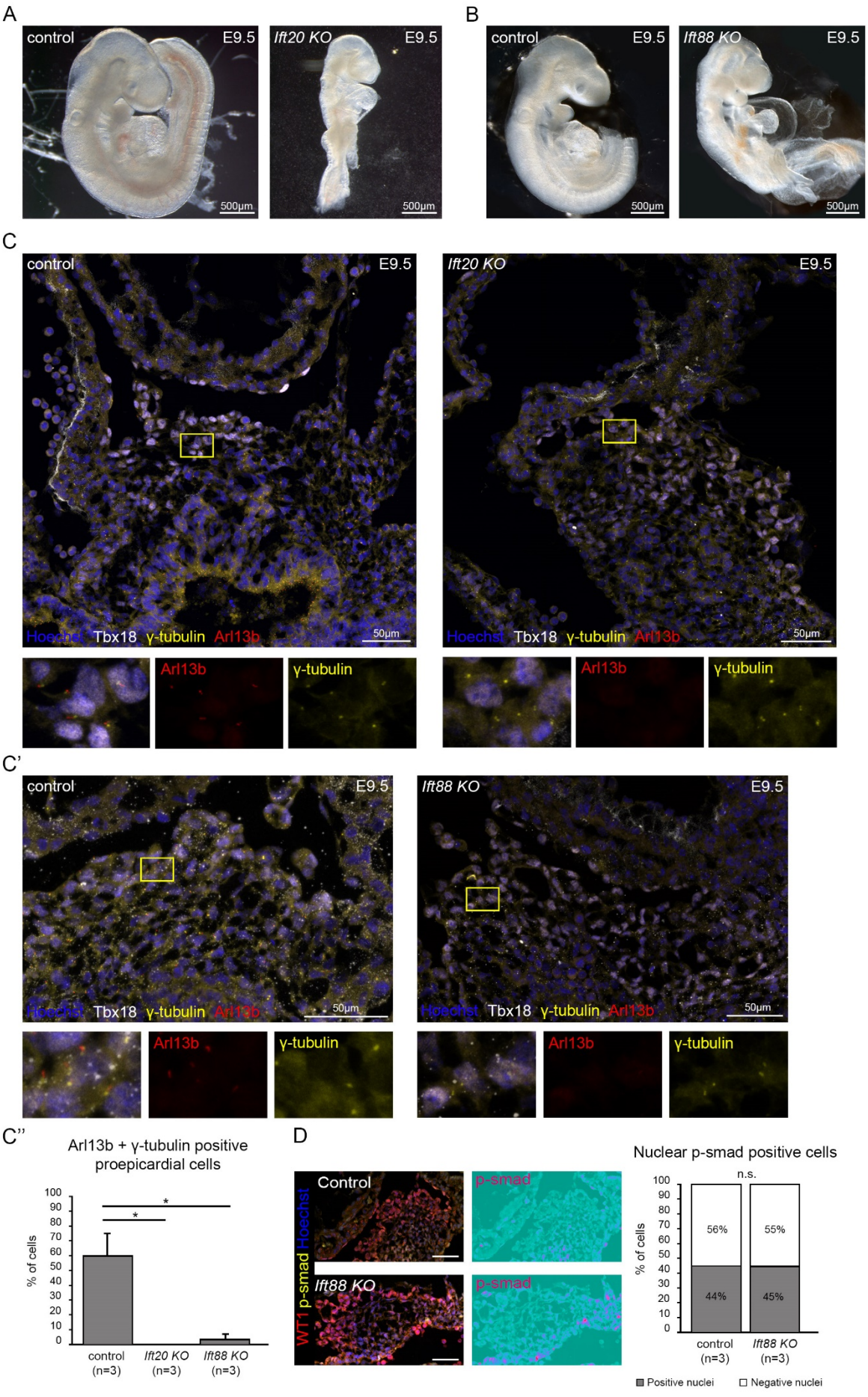
A
control
E9.5
500µm
Ift20 KO
E9.5
500µm
B
control
E9.5
500µm
Ift88 KO
E9.5
500µm
C
control
E9.5
Hoechst Tbx18 γ-tubulin Arl13b
50µm
Arl13b
γ-tubulin
Ift20 KO
E9.5
Hoechst Tbx18 γ-tubulin Arl13b
50µm
Arl13b
γ-tubulin
C'
control
E9.5
Hoechst Tbx18 γ-tubulin Arl13b
50µm
Arl13b
γ-tubulin
Ift88 KO
E9.5
Hoechst Tbx18 γ-tubulin Arl13b
50µm
Arl13b
γ-tubulin
C''
Arl13b + γ-tubulin positive proepicardial cells
% of cells
100
90
80
70
60
50
40
30
20
10
0
*
*
control (n=3)
Ift20 KO (n=3)
Ift88 KO (n=3)
D
Control
p-smad
WT1 p-smad Hoechst
Ift88 KO
p-smad
Nuclear p-smad positive cells
n.s.
% of cells
100
90
80
70
60
50
40
30
20
10
0
56%
55%
44%
45%
control (n=3)
Ift88 KO (n=3)
Positive nuclei
Negative nuclei

Figure S3. Ift20 KO mice proepicardial cells lack cilia. Related to Figures 1 and 2.

(A,B) *Ift20 and Ift88 KO mice show left-right patterning defects including heart looping defects at E9.5.* ***(C)*** *Control and Ift20 KO cryosections imaged by confocal microscopy after labelling with anti-TBX18 (white), anti-Arl13b (red) and anti-γ-tubulin (yellow) antibodies and Hoechst (blue) at E9.5. Zoomed region (enclosed in yellow box) shows the lack of Arl13b signal in Ift20 KO mice. Individual channels are shown for Arl13b (red), γ-tubulin (yellow).* ***(C')*** *Control and Ift88 KO cryosections labelled with anti-TBX18 (white), anti-Arl13b (red) and anti-γ-tubulin (yellow) antibodies and Hoechst (blue) at E9.5. Zoomed region (enclosed in yellow box) shows the decrease of Arl13b signal in Ift88 KO mice. Individual channels are shown for Arl13b (red), γ-tubulin (yellow).* ***(C'')*** *Graph shows the percentage of ciliated PE cells in Ift20 KO (n=3, Ift88 KO (n=3) and control (n=3) mice. The percentage of ciliated PE cells is severely reduced in Ift20 KO (n=3) and Ift88 KO (n=3) when compared to control (n=3) mice. (t-test Ift20 p-value 0.024; t-test Ift88 p-value 0.025). Error bars indicate standard deviation.* ***(D)*** *Control and Ift88 KO cryosections labelled with WT1 (red), p-smad 1/5/9 (yellow) and Hoechst (blue) at E9.5. Individual channel is displayed for p-smad 1/5/9 as ice LUT to facilitate the visualization of signal intensity (green is the minimum and red is the maximum).Graph shows that the percentage of p-smad 1/5/9 positive PE cells is similar in Ift88 KO (n=3 embryos: 1477 nuclei analyzed) and controls (n=3 embryos: 1514 nuclei analyzed) (Chi-square test* of homogeneity *=0.15225, p-value 0.6964 on 1 degree of freedom).*

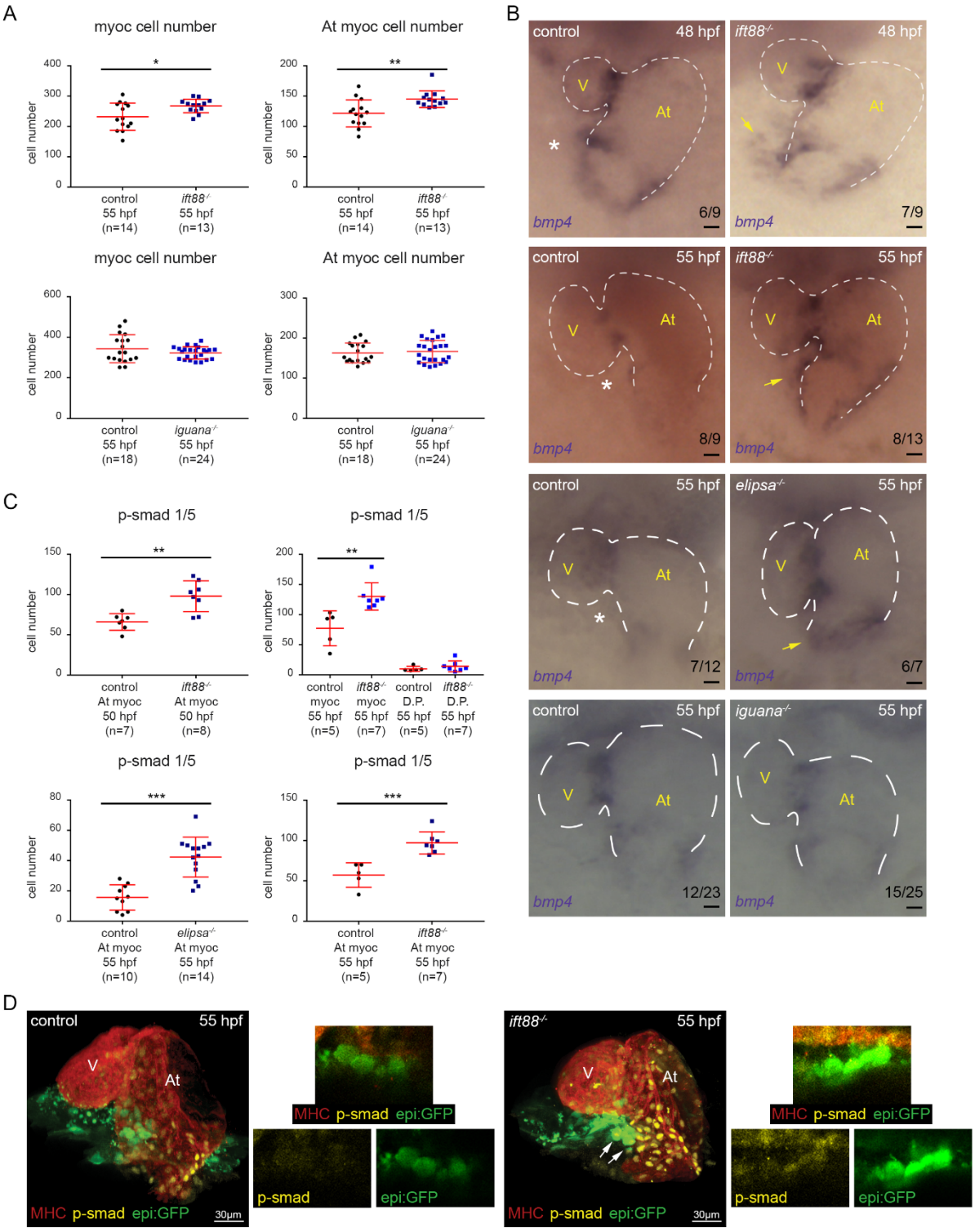

Figure S4. bmp4 is overexpressed in ift88, elipsa/ift54 and Ift20 mutants. Related to Figure 2.

(A) *The top two graphs show total myocardial and atrial-myocardial cell numbers quantified in ift88 (n=13) mutants and controls (n=14) at 55 hpf. (t-test total myocardium p-value 0.016;*

atrial myocardium p-value 0.003). The bottom two graphs show total myocardial and atrial-myocardial cell number quantified in iguana (n=24) mutants and controls (n=18) at 55 hpf. (t-test total myocardium p-value 0.2; atrial myocardium p-value 0.68). ***(B)*** *Whole mount bmp4 in situ hybridization performed on control and ift88 mutant embryos at 48 hpf and at 55 hpf on ift88, elipsa and iguana mutants and their controls. Yellow arrows point to bmp4 overexpression, while white asterisks mark reduced or absent expression. Ventral views, anterior is to the top. V, ventricle; At, atrium. Scale bars 20 µm.* ***(C)*** *Graphs show number of p-smad1/5 positive cells in the atrial myocardium quantified in ift88 (at 50 hpf n=8; at 55 hpf n=7), elipsa (n=14) mutants and their controls (n=7; n=5; n=10 respectively). At 50 hpf, ift88 mutants show p-smad 1/5 increased cell number on the atrial myocardium (t-test p value 0.0017). Similar data were obtained at 55 hpf (t-test p value 0.0008). At 55 hpf, elipsa mutants also show p-smad 1/5 increased cell number in the atrial myocardium (t-test p value 0.0003). At 55 hpf, ift88 mutants show p-smad 1/5 increased cell numbers in the myocardium (t-test p value 0.005).* ***(D)*** *3D projections of whole mount immunofluorescence of hearts using anti-myosin heavy chain antibody (MHC) (red), epi:GFP (green) and anti-p-smad1/5 (yellow) antibody. Arrows mark avcPE cells positive for epi:GFP and p-smad1/5. Zoomed confocal sections show avcPE in ift88 mutant and control embryos. Individual channels are displayed for p-smad 1/5 and GFP. Ventral views, anterior is to the top. In all graphs, red bars indicate mean ±standard deviation.*

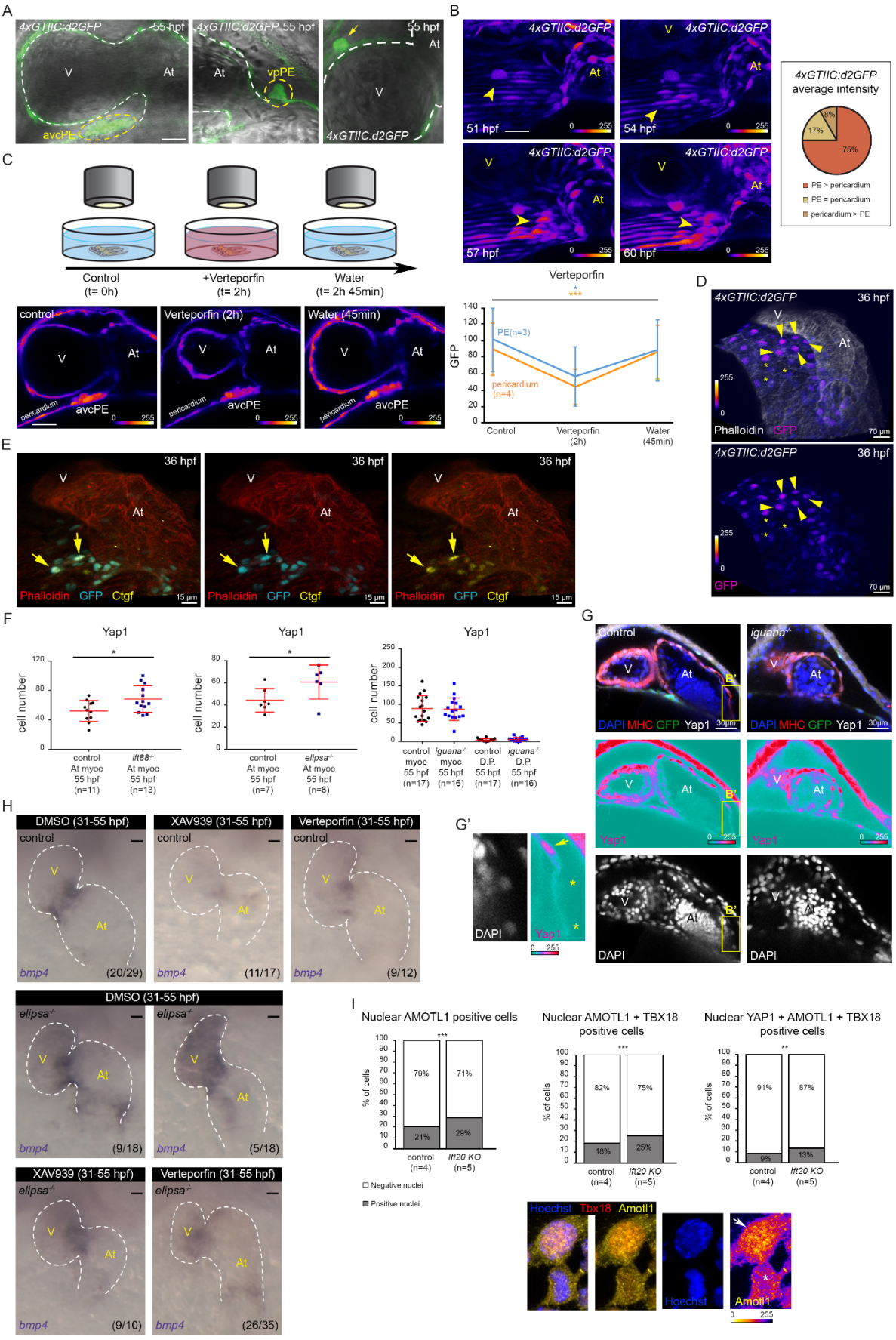

Figure S5 Yap1 activity is increased in the myocardium of ift88 and elipsa/ift54 zebrafish

mutants and AMOTL1 activity is increased in IFT20 KO mice proepicardium. Related to Figure 3.

(A) *Confocal sections of 4xGTIIC:d2GFP signal merged with bright-field, showing Yap/Wwtr1-Tead interaction in avcPE, vpPE, epicardial, myocardial and pericardial cells (n=12). Yellow dashed circles enclose the avcPE and the vpPE. Arrow shows an epicardial cell. Scale bar 20 µm.* ***(B)*** *Maximum projection 4xGTIIC:d2GFP time lapse (51-60 hpf) snapshots (n=6). Arrowheads point at the avcPE. GFP signal is shown as fire LUT where blue is the minimum and yellow is the maximum to facilitate visualization of the intensity changes through the experiment. Scale bar 20 µm. Graph shows 75% of the embryos displayed higher average GFP intensity in PE cells than in pericardial cells (n=12, 7-15 cells of each type).* ***(C)*** *Scheme of the experiment to assess Verteporfin specificity. Time lapse performed on 4xGTIIC:d2GFP embryos at 55 hpf. Yap/Wwtr1-Tead activity (average GFP intensity) was measured on the same PE (3 cells in each embryo, n=3) and pericardial (3 cells in each embryo, n=4) cells at three timepoints: before adding Verteporfin (5µM) (t=0h), after 2 hours of treatment (t=2h) and 45 min after washing out the Verteporfin with fish water (t=2h45 min). Graph shows the decrease in Yap/Wwtr1-Tead activity due to Verteporfin treatment on PE (blue) and pericardial (orange) cells, which is rescued after removing the inhibitor. (Pericardial cells ANOVA p value 0.0007. PE cells ANOVA p value 0.05). Example of 4xGTIIC:d2GFP embryo confocal sections used for the experiment. GFP signal is shown as fire LUT. Scale bar 20 µm.* ***(D)*** *3D projection of 4xGTIIC:d2GFP signal and phalloidin (white) at 36 hpf. GFP signal is shown as fire LUT. Yellow arrowheads show pericardial cells with stronger GFP intensity. Asterisks show pericardial cells with weaker GFP intensity. Individual GFP channel is displayed to facilitate visualization of the dorsal pericardium.* ***(E)*** *3D projection of tcf21:nls-EGFP signal,phalloidin (red) and Ctgf (yellow) at 36 hpf. Yellow arrows show Ctgf and GFP double-positive pericardial cells. Individual channels are*

displayed for GFP (cyan) and Ctgf (yellow) with phalloidin (red). ***(F)*** *The graphs show number of Yap1+ cells in the atrial myocardium (myoc) quantified in ift88$^{-/-}$, epi:GFP (n=13) and elipsa$^{-/-}$, epi:GFP (n=6) mutants and their controls (n=11 and n=7 respectively) at 55 hpf. Mutants show increased Yap1+ cell numbers (t-test ift88 p value 0.024 and elipsa p value 0.042). The last graph shows number of Yap1+ cells in the myoc and dorsal pericardium (D.P.) quantified in iguana$^{-/-}$, epi:GFP (n=16) mutants and their controls (n=17) at 55 hpf (t-test myoc p value 0.875 and D.P. p value 0.312).* ***(G)*** *Control and iguana$^{-/-}$, epi:GFP immunofluorescence (IF) confocal sections labelled with anti-myosin heavy chain antibody (MHC) (red), GFP (green), anti-Yap1 antibody (white) and DAPI (blue) at 55 hpf. Individual channels are displayed for Yap1 (signal is shown as ice LUT to facilitate visualization of signal intensity, where green is the minimum and red is the maximum) and DAPI (white).* ***(G')*** *Zoomed region (yellow box in panel* ***G****) shows Yap1 and DAPI channels to illustrate the method used to quantify Yap1+ (Yap1 signal in the nucleus: yellow arrow) and –negative (yellow asterisks) cells.* ***(H)*** *Whole mount bmp4 in situ hybridization in untreated elipsa mutant (n=18) and control (n=29) embryos and treated with XAV939 (10µM) (elipsa mutant, n=10 and control, n=17) or Verteporfin (20µM) (elipsa mutant, n=35 and control, n=12) from 31 to 55 hpf. Treated embryos showed either decreased or absent bmp4 expression at the atrioventricular canal myocardium and the venous pole. Scale bars 20 µm.* ***(I)*** *Graphs show the percentages of AMOTL1-positive PE cells, double AMOTL1-TBX18-positive PE cells and triple YAP1-AMOTL1-TBX18-positive PE cells in Ift20 KO (n=5 embryos: 1196 nuclei analyzed) and control (n=4 embryos: 929 nuclei analyzed) mice at E9.5. The percentage of nuclear AMOTL1-positive cells (Chi-square test* of homogeneity *= 14,748, p-value 1,23E-04 on 1 degree of freedom), nuclear AMOTL1-TBX18-positive cells (Chi-square test* of homogeneity *= 12,506, p-value 4,06E-04 on 1 degree of freedom) and nuclear YAP1-AMOTL1-TBX18-positive cells (Chi-square test* of homogeneity *= 6,9059, p-value 8,59E-03 on 1 degree of freedom) were*

higher in Ift20 KO than in control mice. Control (n=4) and Ift20 KO (n=5) sections labelled with TBX18 (red), Amotl1 (yellow) and Hoechst (blue). Individual AMOTL1 channel shows the difference between nuclear AMOTL1-positive cells (white arrow) and AMOTL1-negative cells (white asterisk). AMOTL1 signal is shown as fire LUT. In all the images ventral views, anterior is to the top. V, ventricle; At, atrium. In all graphs, red bars indicate mean ±standard deviation.

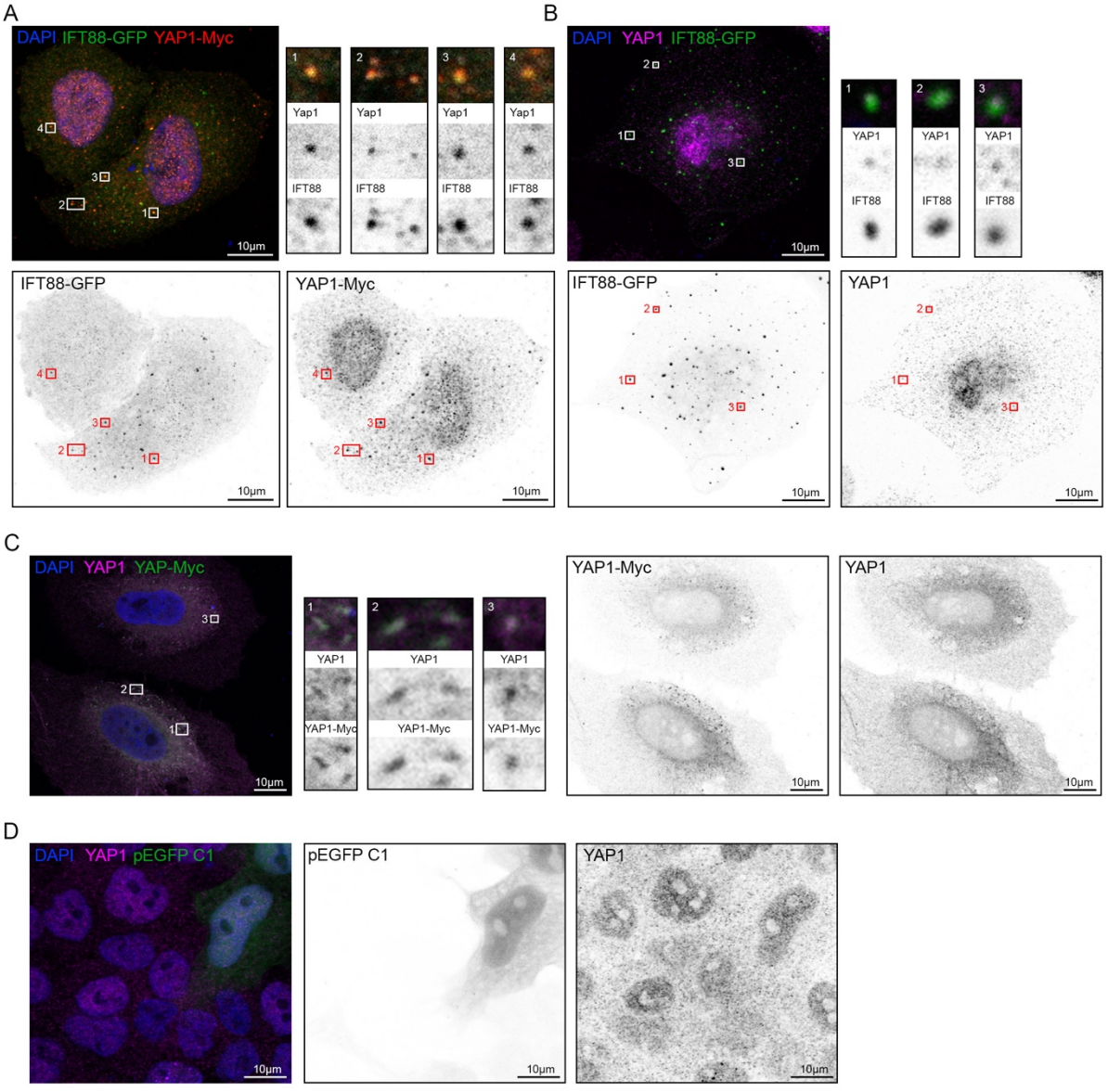

Figure S6. IFT88-GFP co-localize with YAP1 in the cytoplasm. Related to Figure 4.

(A) *Confocal section of HeLa cells transfected with IFT88-GFP and Yap1-Myc plasmids (48h). DAPI (blue), IFT88-GFP (green) and Yap1 (visualized using anti-Myc antibody) (red).*

Individual channels are displayed for IFT88-GFP and Yap1-Myc. ***(1-4)*** *Zoom of selected areas inside boxes showing co-localization.* ***(B)*** *Confocal sections of HeLa cells transfected with IFT88-GFP (48h) showing co-localization with endogenous YAP (visualized using anti-YAP/WWTR1 (TAZ) antibody). DAPI (blue), IFT88-GFP (green) and YAP1 (magenta).* ***(1-3)*** *Zoom of the selected areas inside white boxes showing co-localization of IFT88 and YAP1. Individual channels are displayed for IFT88-GFP and YAP1 signals.* ***(C)*** *Confocal sections of HeLa cells transfected with Yap1-Myc (48h) showing co-localization with endogenous YAP1 (visualized using anti-YAP/WWTR1 (TAZ) antibody). DAPI (blue), Yap1-Myc (green) and YAP1 (magenta).* ***(1-3)*** *Zoom of the selected areas inside white boxes showing examples of co-localization between Yap1-Myc (visualized using anti-Myc antibody) and endogenous YAP1 (using YAP/WWTR1 (TAZ) antibody) signals. Individual channels are displayed for Yap1-Myc and YAP1 signals.* ***(D)*** *Confocal sections of HeLa cells transfected with pEGFP C1 (48h) do not show co-localization with endogenous YAP1 (visualized using anti-YAP/WWTR1 (TAZ) antibody). DAPI (blue), pEGFP C1 (green) and YAP1 (magenta). Individual channels are displayed for pEGFP C1 and YAP1 signals.*

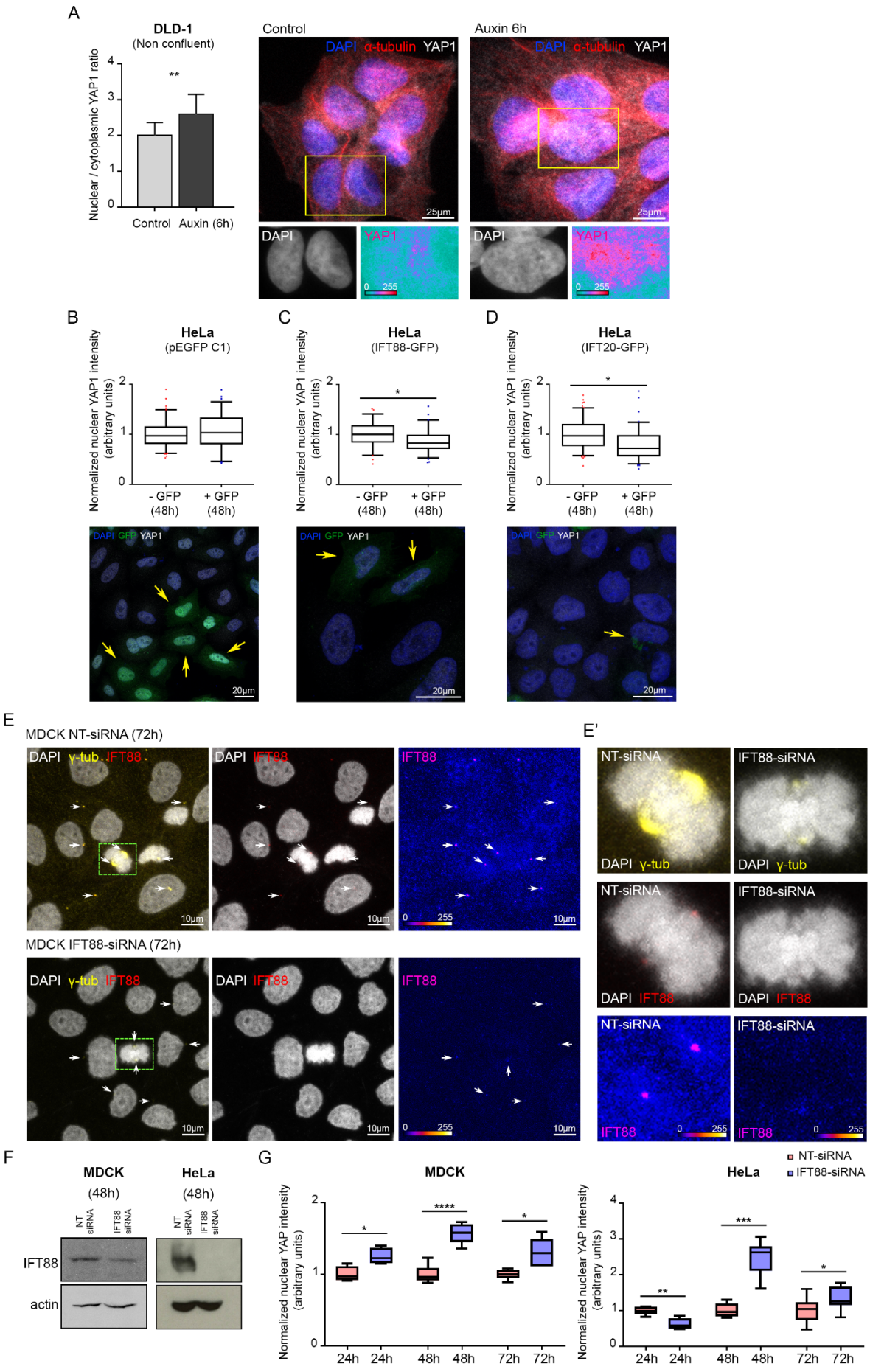
A
DLD-1
(Non confluent)
Nuclear / cytoplasmic YAP1 ratio
Control
Auxin (6h)
**
Control
Auxin 6h
DAPI α-tubulin YAP1
25µm
DAPI
YAP1
0 255
B
C
D
HeLa
(pEGFP C1)
(IFT88-GFP)
(IFT20-GFP)
Normalized nuclear YAP1 intensity (arbitrary units)
- GFP (48h)
+ GFP (48h)
*
DAPI GFP YAP1
20µm
E
MDCK NT-siRNA (72h)
MDCK IFT88-siRNA (72h)
DAPI γ-tub IFT88
DAPI IFT88
IFT88
10µm
E'
NT-siRNA
IFT88-siRNA
DAPI γ-tub
DAPI IFT88
F
MDCK
(48h)
HeLa
(48h)
NT siRNA
IFT88 siRNA
IFT88
actin
G
MDCK
HeLa
NT-siRNA
IFT88-siRNA
Normalized nuclear YAP intensity (arbitrary units)
24h 24h 48h 48h 72h 72h
*
**
***
****

Figure S7. IFT88 and IFT20 regulate YAP1 activity. Related to Figure 4.

(A) *YAP1 nuclear/cytoplasmic ratio is increased in cells treated with auxin (6h) (Mann-Whitney p-value 0.004). (controls: 2 replicates, n=102 cells; Auxin 6h: 2 replicates, n=104 cells). Error bars indicate standard deviation. Immunofluorescence (IF) confocal images of DLD-1 cells treated with auxin (6 h) and controls. DAPI (blue), YAP1 (white) and α-tubulin (red). Zoomed regions show DAPI and YAP1 channels. YAP1 channel is shown in ice LUT where green is the minimum and red is the maximum to facilitate the visualization of signal intensity increases after treatment.* ***(B-D)*** *IFT88 and IFT20 overexpression assays performed in HeLa cells (48h). Graphs show nuclear YAP/WWTR1 (TAZ) signal in GFP-positive cells (+ GPF), compared to GFP-negative cells (- GPF: endogenous control) in cells transfected with pEGFP C1 (GFP control) (n=4 replicates, average cell number analyzed for each condition = 22, t-test p-value 0.5)* ***(B)****, IFT88-GFP (n=3 replicates, average cell number analyzed for each condition = 23, t-test p-value 0.01)* ***(C)*** *or IFT20-GFP (n=4 replicates, average cell number analyzed for each condition = 27, t-test p-value 0.03)* ***(D)****. Box and whiskers (5-95 percentile). Outliers are represented as red dots (-GFP) or blue squares (+GFP). IF confocal images of cells transfected with pEGFP C1 (GFP control), IFT88-GFP or IFT20-GFP. DAPI (blue) and YAP/WWTR1 (TAZ) (white). Yellow arrows mark GFP signal.* ***(E)*** *IF confocal images of MDCK cells treated with NT- or IFT88-siRNA (72h). DAPI (white), γ-tubulin (yellow) and IFT88 (red). White arrows highlight IFT88-positive centrosomes facilitating the visualization of IFT88 signal depletion upon IFT88-siRNA treatment.* ***(E')*** *Zoom of dividing cells (green boxes) treated with NT-siRNA and IFT88-siRNA respectively. Centrosomes show reduced IFT88 (red) and γ-tubulin (yellow) signal after IFT88 depletion. DAPI (white). IFT88 channel is shown in fire LUT where blue is the minimum and yellow is the maximum to facilitate the visualization of the intensity reduction after the treatment.* ***(F)*** *Western blot analysis of HeLa and MDCK cells after 48h NT- and IFT88-siRNA treatments respectively.* ***(G)*** *Graphs*

show the increase in nuclear YAP/WWTR1 (TAZ) signal in IFT88-siRNA treated cells (blue), compared to NT-siRNA controls (red) at 24, 48 and 72h. Box and whiskers (5-95 percentile). (MDCK: 24h: n=1 replicate, average cell number analyzed for each condition = 42, t-test p-value 0.02; 48h: n=1 replicate, average cell number analyzed for each condition = 52, t-test p-value <0.0001; 72h: n=1 replicate, average cell number analyzed for each condition = 126, t-test p-value 0.01) (HeLa: 24h: n=1 replicate, average cell number analyzed for each condition = 12, t-test p-value 0.001; 48h: n=1 replicate, average cell number analyzed for each condition = 12, t-test p-value 0.0002; 72h: n=1 replicate, average cell number analyzed for each condition = 32, t-test p-value 0.047).

Average intensity	Embryo_01	Embryo_02	Embryo_03	Embryo_04	Embryo_05	Embryo_06
PE cells	71,37	72,42	30,84	89,57	69,72	49,63
St-Dev	11,91	21,49	26,85	20,56	24,85	13,35
Pericardial cells	52,45	45,17	55,81	94,08	49,98	29,95
St-Dev	21,16	9,76	18,25	29,84	14,67	7,51
t-test	**0,0325**	**0,0084**	0,0101	0,7309	0,0608	**0,0001**

Average intensity	Embryo_07	Embryo_08	Embryo_09	Embryo_10	Embryo_11	Embryo_12
PE cells	63,69	60,99	115,45	64,67	56,23	107,03
St-Dev	26,92	18,28	6,52	11,43	10,46	21,14
Pericardial cells	28,76	31,59	74,03	36,44	30,05	68,40
St-Dev	16,68	7,78	22,14	6,82	8,85	28,52
t-test	**0,0055**	**0,0005**	**0,0001**	**0,0000**	**0,0002**	**0,0024**

Table S1. Yap/Wwtr1-Tead activity (GFP average intensity) in PE and pericardial cells. Related to Figure 3.

Statistically significant results are highlighted in bold.